Chapter 9

Synthesis and Properties of Silver Filled Carbon Nano-cables

Abstract

We present a method for fabricating large quantities of carbon nanotubes (CNTs) filled with pure silver using a hydrogen arc. The growth mechanism is proposed to proceed within a phase diagram approach. The size-dependent electronic structures of these materials were investigated using electron energy loss spectroscopy (EELS), and the surface plasmon and bulk-excitation character are discussed. A liner current-voltage (*I*-*V*) characteristic with resistance of ~37 kΩ was obtained in a nanocable. The structure is similar like coaxial nanocable geometry and also suggests applications in nanoscale of electronics, optical device and biochemsensors.

9.1 Introduction

One-dimensional (1D) nanostructured materials including nanowires, nanorods, nanobelts, nanotubes and nanocables have attracted much attention in recent years due to their unique properties and potential applications in electronic and photonic devices.[1,2,3] One-dimensional nanomaterials also provide an ideal model system to investigate physical phenomena such as quantized conductance and localization effects.[1,4] In particular, silver nanowires are interesting to study because bulk silver possesses the highest electrical conductivity and thermal conductivity, and it has been used in a verity of commercial applications. In most of these applications, the performance of silver could be potentially enhanced by processing it into one-dimensional nanostructures.[5] For example, Ag

nanostructures, with their large surface to volume ratio, are used to study surface plasmon resonances (SPR) and surface-enhanced Raman scattering (SERS) with applications in biosensing.[6,7]

Carbon naontubes (CNT), with their unusual properties[8] and the potential for applications,[9,10] have been prepared by a variety of methods, including: arc-discharge,[11] laser ablation,[12] chemical vapor deposition (CVD).[13] For example, the development of nanoscale biosensor and bioreactor systems based on CNT has been driven by the experimental evidence that biological species such as proteins and enzymes can be immobilized on the surface of CNT.[9] CNT also exhibits highly attractive capillary properties.[14] For instance, it has been demonstrated that many interesting materials could be made by filling the hollow spaces inside the CNT. Several approaches showed that when CNT heated in the presence of metal (M) and metal oxide (MO_x), these materials can filled the inside of the CNT forming a coaxial nanostructure which we term here M(or MO)@C nanocable. The first observation of MO@C nanocable was reported by Ajayan and Iijima.[15] Their method involved the arc evaporation of a composite carbon electrode made by mixing graphite powder with metals or metal oxides.[16] In 1994, Ajayan et al. showed that long pure Mn@C nanocable can be formed by doping the anode with pure Mn metal.[17] Pascard reported carbon nanotubes filled with various transition metal have been formed in a helium arc.[18] Pure Cu@C and Ge@C nanocable have been synthesized using a hydrogen arc.[19] A number of methods have been developed to generate Ag@C nanocable: de Heer synthesized Ag@C nanocables by draw in molten metal nitrates into CNTs which reduce to pure metal inside the nanotube upon heating;[20] Green et al. reported a liquid phase method KCl-UCl_4 and AgCl-AgBr to fill single-wall carbon nanotubes (SWCNTs);[21] Rao et al. employed a sonochemical means to fabricate silver metal in SWCNT;[22] Li et al. have fabricated silver filled CNT structure by hydrothermal method.[23]

We report in this article the successful use of carbon black with silver powders as a starting material to produce high density and high purity Ag@C nanocables. Using an array of

electron probe tools we studied the structure and the electronic properties of the nanocables. The results of these studied are reported below.

9.2 Experimental Section

The Arc system used in this study was described in reference.[24] Briefly, the arc consists of two electrodes: the anode is a cup fabricated from a 3/8-in.-diameter rod of randomly oriented graphite (ROG) with a hole of 3/16 in. diameter are 3/8 in. in depth. The cathode is a solid 3/8-in.-diameter ROG rod. The hole in the anode cup is filled with a tightly compacted carbon black (Alfa Aesar, 200 mesh, 99.99 %) mixed with 10 ~ 50 atomic percent of Ag powder or pure Ag powder (Inframat Advanced Materials, 150 nm, 99.95%) and Ag rod (Alfa Aesar, 99.99 %). The arc is formed by a dc supply (100 A, 20 ~ 30 V) under a pure hydrogen atmosphere at an operating pressure in the range of 100 ~ 500 torr and it is maintained by adjusting the electrodes spacing between 0.5 to 0.7 in. A typical synthesis experiment between 30 s to 3 mins. The powder deposit formed on the cathode side after the arc experiment contains Ag@C nanocables of 80 % yields and nanoparticles. The powder sample is dispersed in ethanol using an ultrasonic instrument and a lacey carbon grid is used to shipment the nano speciment for electron microscopy observations.

SEM images were obtained by using a Hitachi S-4500 field emission scanning electron microscope (FESEM) operated at an acceleration voltage of 15 kV. Transmission electron microscope (TEM), selected area electron diffraction (SAED), energy-dispersive X-ray spectroscopy (EDXS), electron energy loss spectroscopy (EELS) and scanning transmission electron microscope (STEM) studies are performed using a JEOL 2100 FASTEM working at 200 kV, equipped with a Gatan slow scan charge-coupled device (CCD) camera, Oxford INCA EDXS and Gatan EELS attachments. The electrical measurement of the nanocable was made by the dc two-terminal method at room temperature.

9.4 Results and Discussion

The SEM observation is carried out to investigate the morphology of nanocable. Figure 9.1 (a) shows a typical SEM image of Ag@C nanocable bundles synthesized by arc discharge method. It is estimated that the diameters of the nanocables ranged from 30 to 145 nm and most of nanocables are about 100 nm. These nanocables are 6 to 20 μm in lengths. From the enlarged image, we find that tips of the Ag@C nanocables are terminated with nano particles which consist of carbon and silver compare to that of nano cable are measured by EDXS the same with nanocable. We also notice that these are nanocables that are not completely filled with Ag as marked by white arrow in Figure 9.1 (b). We also made Ag@C nanocables by using pure Ag powder which was packed in the hole of anode as precursor and can get 95 % Ag nanocables in yield in Figure 9.1 (c). Those nanocables have diameter range from 160 ~ 240 nm and up to several tens μm in length. If we change to use pure Ag rod as presursor, huge Ag@C nanocable with 350 ~ 580 nm in diameter and reaching 100 μm in length can receive.

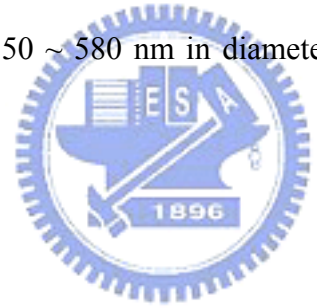

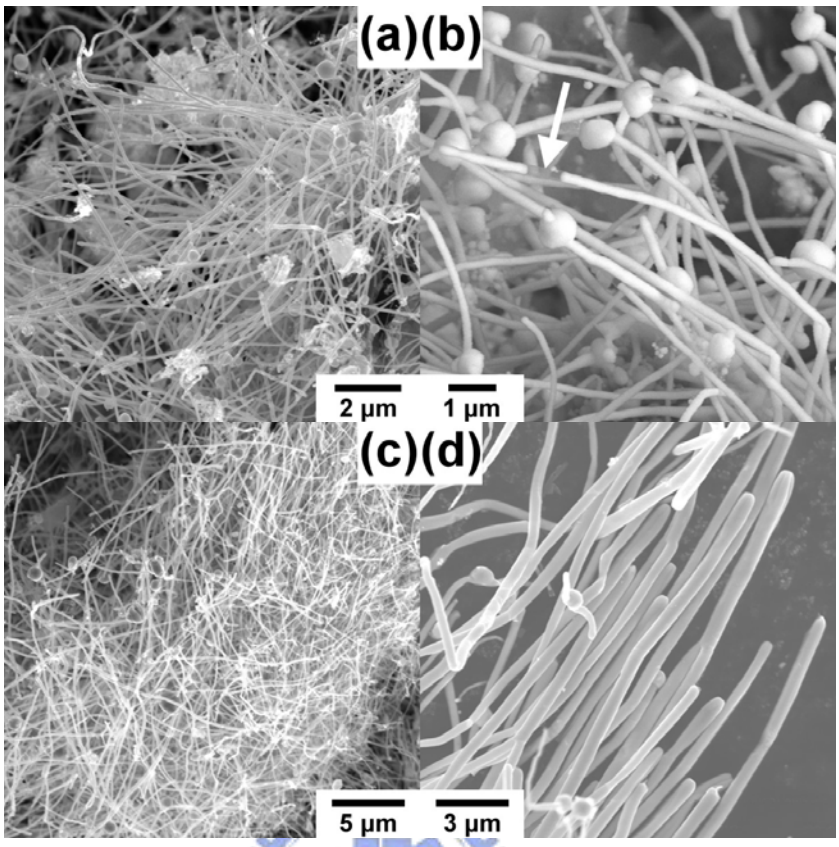

Figure 9.1 (a) SEM image of Ag@C nanocable bundles synthesized by 10 % Ag powder with carbon black using arc discharge method. (b) Enlarge image of nanocable tip. (c) Ag@C nanocables synthesized by pure Ag powder. (d) Ag@C nanocables synthesized by pure Ag rod.

The TEM images of Ag@C nanocables are show in Figure 9.2. Figure 9.2 (a) shows a 5 μm long Ag@C nanocable with a diameter of 55 nm and is completely filled with Ag. The nanocable is connected to a 400 nm diameter nano particle and which also consists of carbon and silver. In Figure 9.2 (b), a bundle of tangled Ag@C nanocables is shown. We notice that a nanoparticle is often found at the tip. As the shape of the tips, no sharp-cone caps are found and the terminations are rather smooth, round and always encapsulated by carbon shell. A straight, uniform, crystalline and without defect Ag@C nanocable was observed in Figure 9.2 (c), the diameter of the nanocable is approximately 80 nm. It shows that the nanocable has a crystalline core and surrounding graphite sheets. Figure 9.2 (d), (e) and (f) provide HRTEM

and SAED images of the Ag@C nanocable taken from the white circle of Figure (c), and it directly demonstrates the structure of the nanocable. In Figure 9.2 (e), the distance of between two pair of Ag atom layers is 0.204 nm which further indicate for the growth direction as [100]. The SAED in Figure (f) shows the present of both crystalline Ag and graphite layers with $d_{(002)}$ = 0.34 nm. Such a geometric lattice implies that the corresponding structure belong to the face centered cubic (fcc) phase of silver.

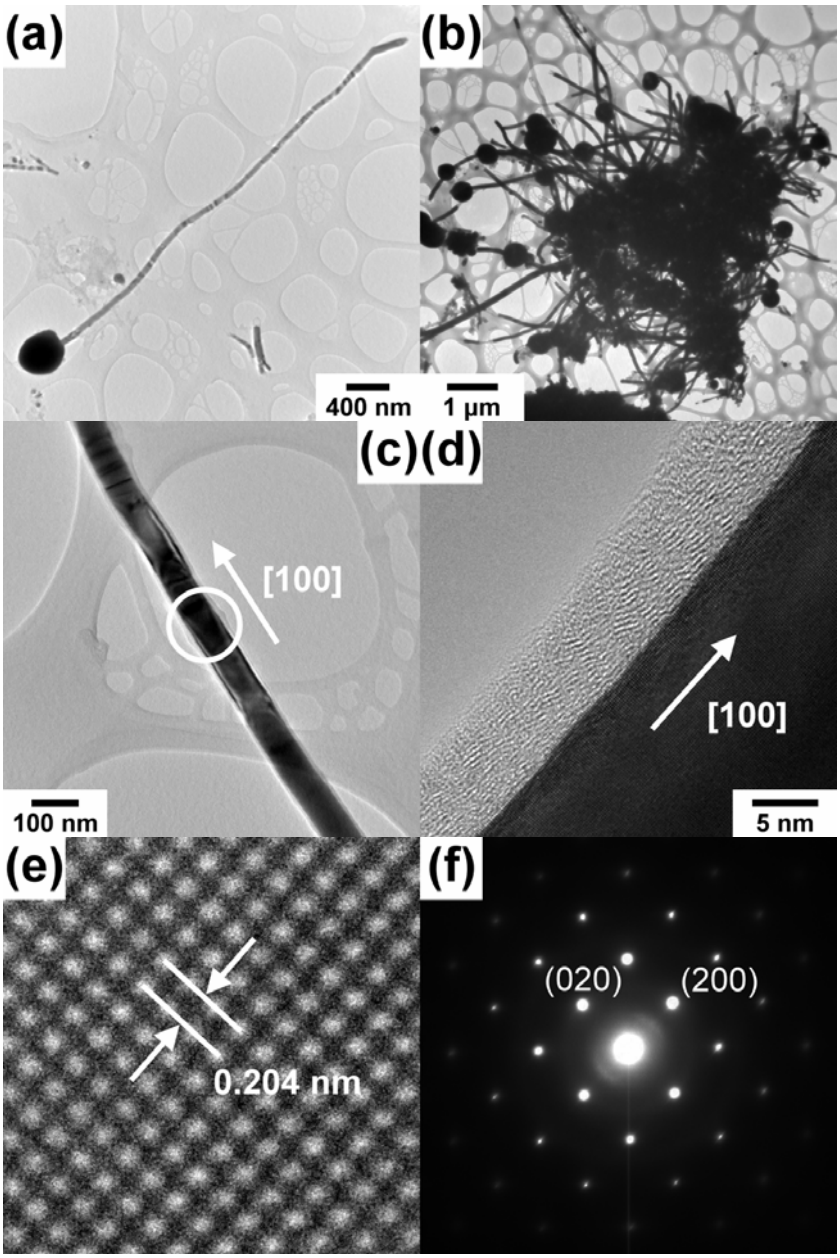

Figure 9.2 Low magnification TEM image of (a) an individual Ag@C nanocable with Ag@C ball and (b) Ag@C nanocable bundle. (c) TEM image of an individual purity single crystalline nanocable. HRTEM images of (d) a Ag@C nanocable with about 6 nm graphite sheets and (e) the core lattice image from (c). (f) The correspondind SAED pattern indicates [100] growth direction.

Figure 9.3 (a) shows a low magnification TEM image of typical Ag@C nanocable prepared by arc discharge method. The light-dark contrast shell surround the nanowire

direction indicates its coaxial structure.[25] Figure 9.3 (b) shows EDXS analysis in nanobeam mode on the central of the nanocable taken from Figure 9.3 (a) indicating that the nanocable is composed of mainly carbon and silver respectively. In order to recognize the coaxial cable-like structure, we observed the nanocable by high angle dark field (HADF) image. This image is formed by collecting high-angle Rutherford forward-scattered electrons, and is in the z-contrast mode. Figure 9.3 (c) shows a typical z-contrast image exhibiting the crystalline core that strongly diffracts electrons appearing as bright of Ag. An elemental profile analysis was performed by scanning focused electron beam across an individual nanocable via a white line route in an attempt to reveal the element concentration distribution shown in Figure 9.3 (d). The Ag profile is homogeneous nanowire in center and the C profile is characteristic of a hollow carbon nanotube sheath (i.e., it starts abruptly, reaches a maximum at the inner radius, and decreases at the center) surrounding a Ag nanowire core.

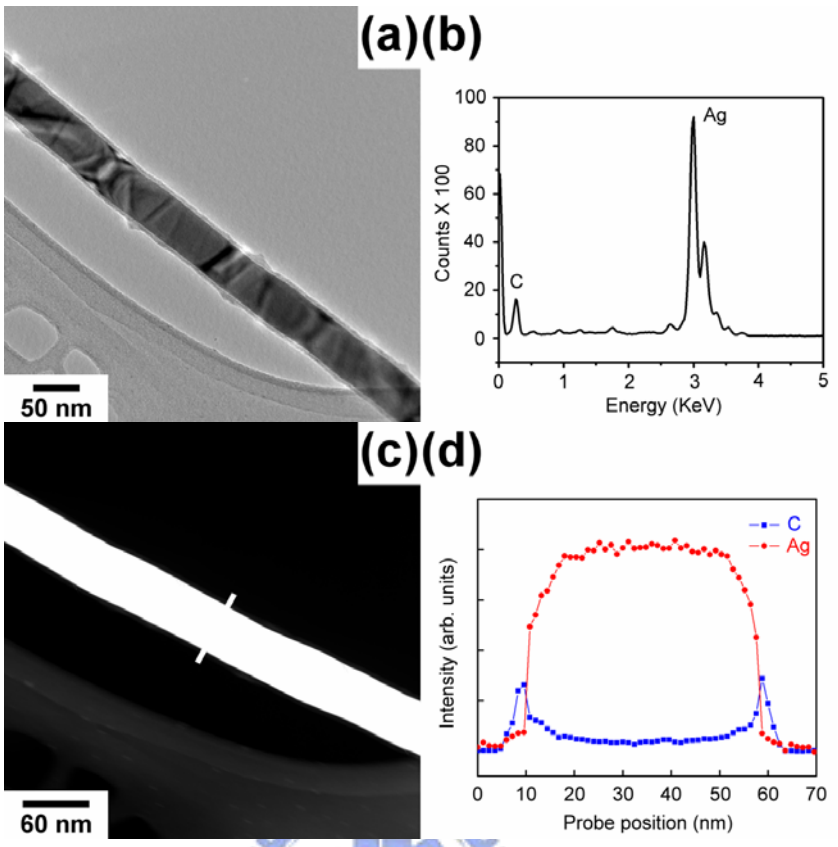

Figure 9.3 (a) A typical TEM image of the Ag@C nanocable with a graphite shell. (b) EDXS indicates the composite of nanocable by C and Ag. (c) The HADF z-contract image made from (a), showing the bright region is Ag and (d) the elemental profile taking across a nanocable.

Figure 9.4 (a) is a SEM image of as-grown CNTs with 10 % yields in 100 torr of hydrogen and with 30 V are voltage, filled by Ag by EDXS studies indicate the nanotubes are not and the bottom of bundle is pure carbon. Figure 9.4 (b) is a low magnification image of hollow CNTs with diameter of 100 nm and the corresponding ED pattern with graphite (002) plane. Figure 9.4 (c) shows a CNT bundle with unfilled Ag nanowire indicating by EDXS, but few nanoparticles. Some of the CNTs are encapsulated by Ag nanoparticles at the tips. The Ag nanoparticles with about 80 % yields we find are only round shape with a variety of diameters from 10 to several hundreds nanometer much smaller than using 20 V. Under this violent condition, graphene sheets crystallized into carbon nanotubes with a rough surface quickly

and didn't have much time to rearrange well. On the other hand, silver also couldn't coalesce and growth into 1-D structure on this environment.

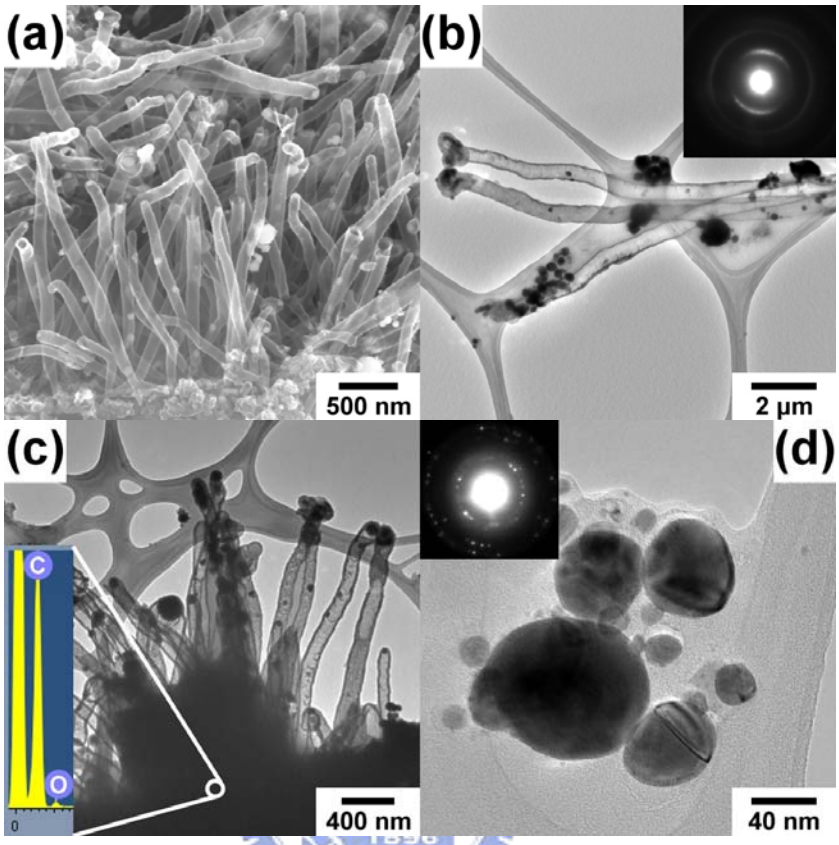

Figure 9.4 The raw materials formed in 100 torr of hydrogen and with 30 V dc (100 A) supply. (a) SEM image of carbon nanotubes unfilled with Ag and the insert EDXS indicates it is made of carbon. Low magnification TEM images of (b) insular CNTs after using supersonic, (c) a CNT bundle and (d) Ag nanoparticles.

The surface plasmon phenomena and chemical composition are studied by EELS. A representative zero-loss EELS spectrum from a Ag@C nanocable with diameter of about 100 nm is shown in Figure 9.5 (a). It presents the Ag plasmon peaks below 40 eV, and the Ag-$N_{2,3}$ edges.[26] Figure 9.5 (b) shows a core-loss EELS spertrum, only the C-K edge (284 eV)[27,28] and the Ag-M edges (395 eV)[27] are present on the spectrum obtained on selected parts of this nanocable. It reveals the direct evidence of K edge peak of inner shell excitation from carbon

shell by incident electron beam.

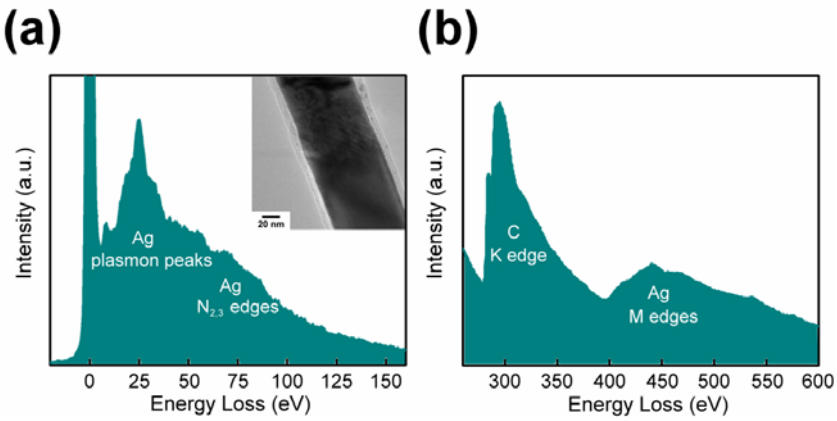

Figure 9.5 Typical EELS spectra were taken from part of a nanoacable with a diameter about 100 nm. (a) zero-loss and (b) core-loss spectrum.

In order to study the Ag@C nanocable surface plasmon, high spatial resolution EELS analyses are performed with 0.05 eV resolution recorded on subnanometer area. We take plasmon EELS spectra from center part of nanocables in Figure 9.5 (a). In Figure 9.6 (a) there are five plasmon peaks revealed. Except the zero peak, we can easily identify a surface plasmon at about 3.8 eV, the surface- and bulk-excitation character at about 8.3 eV.[26b] Three strong higher-energy loss peaks are at about 18.25, 25.55 and 33.85 eV identified as the ionization edges. Figure 9.6 (b) is consistent with the plasmon EELS spectrum taken from an unfilled CNT. It reveals a carbon bulk plasmon at about 24 eV.[26a]

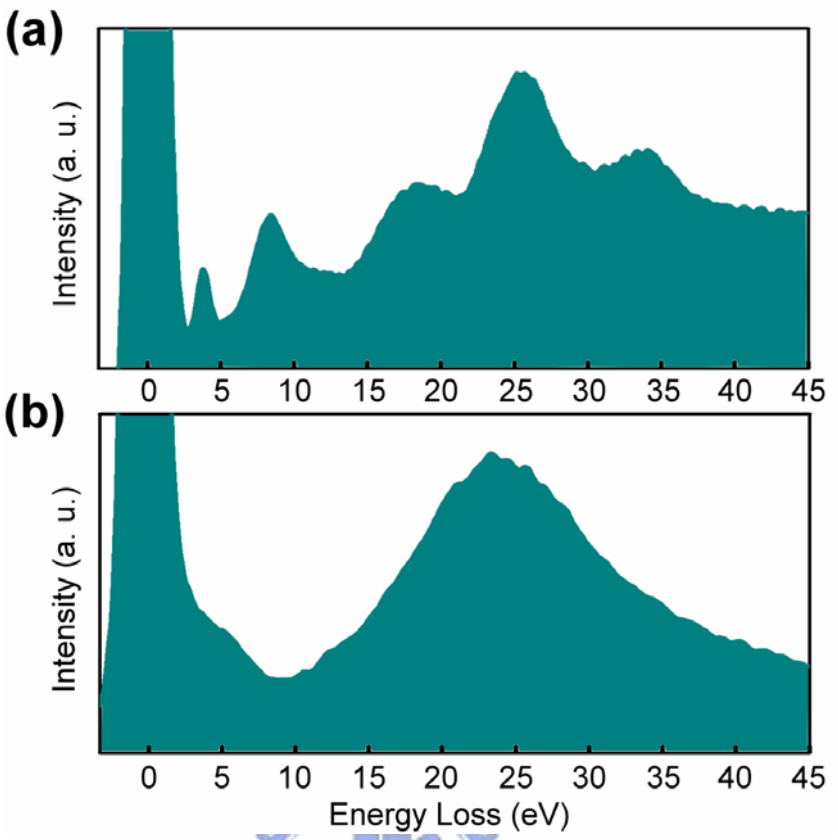

Figure 9.6 EELS plasmon spectra obtained on a part of (a) a pure Ag@C nanocable and (b) a CNT unfilled with Ag.

We have collected plasmon EELS spectra from Ag@C nanocables with different diameters ranging from 42 to 145 nm. The energy of those plasmon peaks are plotted against the diameters of the Ag@C nanocables shown in Figure 9.7. In these plots, we find the surface plasmon peak and bulk-excitation peak of nanocables shift toward the lower energies as diameter decreases from 145 to 42 nm. These red shifts are due to the quantum size effect and the large surface to volume ratio. These effect is similar to the surface plasmon for metal clusters.[26a,29]

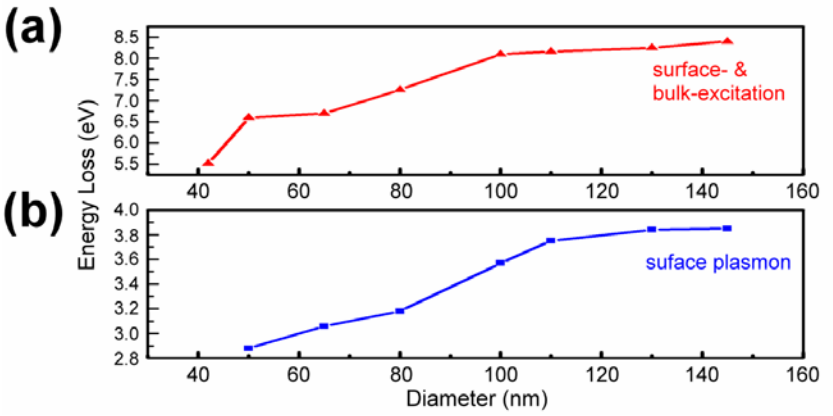

Figure 9.7 The position of the Ag plasmon peaks were plotted against the diameters of the Ag@C nanocables.

We measured the resistance of a typical Ag@C nanocable at room temperature using the two-point contact. The insert image of Figure 9.8 shows a Ag@C nanocable with diameter of ~200 nm and aligned across two gold electrodes. A linear *I-V* characteristic clearly indicates that the electrical contact between the electrodes and the Ag@C nanocable with conductivity with a 0.5 x 10^4 S/cm is calculated. This value should be compared 0.8 x 10^5 S/cm for a silver nanowire[30] and 0.1 x 10^4 S/cm for MWCNTs.[31]

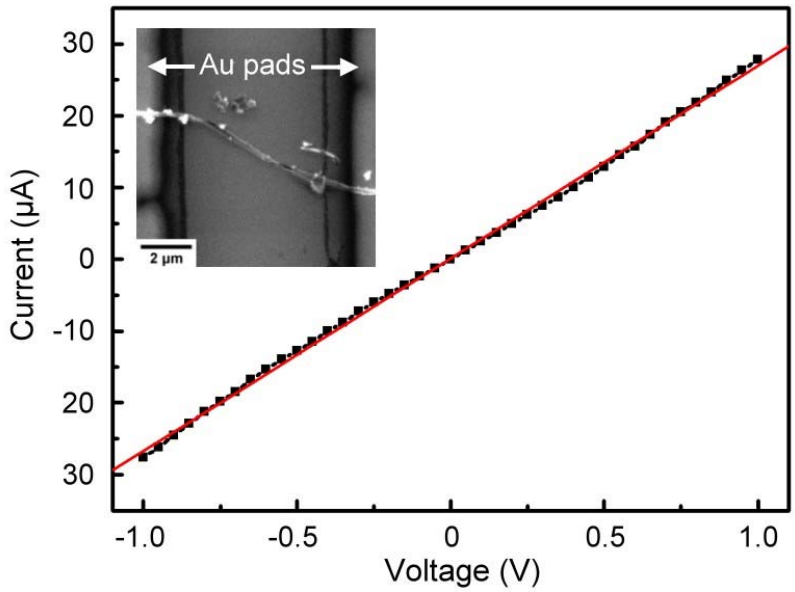

Figure 9.8 The *I-V* property of a Ag@C nanocable. The insert shows a SEM image of an individual nanocable across two parallel gold electrodes.

The experimental results suggest that these Ag@C coaxial nanocable heterstructures are grown via a co-growth vapor transfer mechanism. Silver and carbon are in the vapor phase from high temperature Arc, which is transferred to the lower temperature zone, in which cathode graphite surface provides and condenses together to form the specific coaxial configuration. To understand the observation of Ag@C nanocables in these experiments the following model is proposed. In typical vapor-liquid-solid (VLS) process, one of the most frequently mentioned 1D nanostructure mechanism is proposed in Scheme 9.1.[32] The first step of the process is the formation of components of the nanocables which consisted of silver clusters and particles supersaturated with graphene sheets are evaporated from carbon black.[33] These particles that nucleated under the assistance of a nanosized liquid-phase catalyst may act as seeds, migrate and coalesce at high temperatures. The supersaturation is generated by decomposition, absorption of carbonaceous structure are the surface of the nanoparticles and dissolution in the liquid phase.[34] In general, graphite has a low solubility in the metallic solid phase and metal-rich metallic carbides are unstable or metastable.[35] As a consequence, silver-carbon phase diagrams display in general a eutectic point between the liquid solution, graphite and silver. Upon slow cooling, the solidification involving, simultaneously, the silver and graphite carbon and the solubility limit of carbon decreases and carbon starts to crystallize at the surface of silver. Since carbon has a low surface tension, so that the segregation of graphite carbon can occurs via a diffusion towards the silver surface to the formation of graphite sheets. The significant in our result is that the shell material carbon nanotube was generated in situ as a hard template[36] in the growth of Ag@C nanocables. The carbonaceous via condensation reaction into graphite shells as a template in the process, in situ Ag atom combine into clusters and nanoparticles. By diffusion and coherence at high temperature which was above melting points of silver, the particles combine and restructure crystalline plane into nanosized crystal. Under hydrogen atmosphere, the nanocrystal grows anisotropically with [100] direction into one-dimensional nanocables.

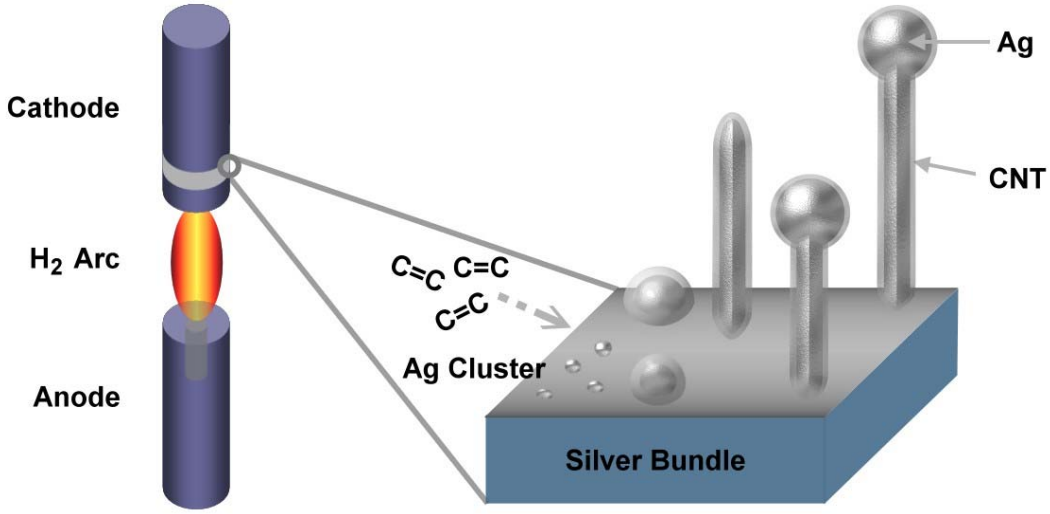

Scheme 9.1 Proposed pathway to form Ag@C nanocables.

9.5 Conclusion

In conclusion, we have demonstrated that large-scale synthesis of 1-D Ag@C nanocables can be grown easily in one step via VLS process. In this process, the development of silver and graphite carbon in to anisotropic structure was mainly driven by two factors: first, the pre-construction of metal seeds under the graphite rod surface could serve as nuclei for the successding growth of Ag@C nanocables; and second, graphite has a much lower solubility in liquid Ag. If we consider a slow cooling process when the cathode surface reaches the solidification temperature, graphene sheets will start to crystallize into graphite layers at the silver surface and also serve as a hard template in this growth process. In simultaneously, silver could crystallize into face centered cubic (fcc) silver within an anisotropic nanostructure.

In the low energy-loss region EELS spectra of Ag@C nanocables with variety of diameters, the energy of surface plasmon peak shifts toward the low energy, as the diameter decreases. This red shift is due to the quantum size effect and in terms ratio of surface to volume. In the resulting of electrical property, nanocable display mid-resistance compared to

silver nanowire and CNTs. The experimental results strongly suggest that these Ag@C naocables are of high electronic quality for optoelectronic nanodevices.

Further more, we believe that it can also bind or absorb with small molecules and protein-DNA for biochemsensors.

References

1. (a) Iijima, S. *Nature* **1991**, *354*, 56. (b) Hu, J.; Odom, T. W.; Lieber, C. M. *Acc. Chem. Res.* **1999**, *32*, 435. (c) Feldman, Y.; Wasserman, E.; Srolovitt, D. J.; Tenne, R. *Science* **1995**, *267*, 222. (d) Kong, J.; Soh, H. T.; Cassell, A. M.; Quate, C. F.; Dai, H. *Nature* **1998**, *385*, 878. (e) Chung, S.-W.; Yu, J.-Y.; Heath, J. R. *Appl. Phys. Lett.* **2000**, *76*, 2068. (f) Dekker, C. *Phys. Today* **1999**, *May*, 22. (g) Frank, S.; Poncharal, P.; Wang, Z. L.; de Heer, W. A. *Science* **1998**, *280*, 1744. (h) Huang, M. H.; Mao, S.; Feick, H.; Yan, H.; Wu, Y.; Kind, H.; Weber, E.; Russo, R.; Yang, P. *Science* **2001**, *292*, 1897.
2. (a) Bachtold, A.; Hadley, P.; Nakanishi, T.; Dekker, C. *Science* **2001**, *294,* 1317. (b) Hong, B. H.; Bae, S. C.; Lee, C. W.; Jeong, S.; Kim, K. S. *Science* **2001**, *294*, 348. (c) Hong, B. H.; Lee, J. Y.; Lee, C.-W.; Kim, J. C.; Bae, S. C.; Kim, K. S. *J. Am. Chem. Soc.* **2001**, *123*, 10748. (d) Ye, C. H.; Meng, G. W.; Jiang, Z.; Wang, G. Z.; Zhang, L. D. *J. Am.Chem. Soc.* **2002**, *124*, 15180.
3. (a) Wang, Z. L. *Adv. Mater.* **2000**, *12*, 1295. (b) Suh, S. B.; Hong, B. H.; Tarakeshwar, P.; Youn, S. J.; Jeong, S.; Kim, K. S. *Phys. Rev. B* **2003**, *67*, 241402(R). (c) Wang, Y. W.; Meng, G. W.; Zhang, L. D.; Liang, C. H.; Zhang, J. *Chem. Mater.* **2002**, *14*, 1773. (d) Nautiyal, T.; Rho, T. H.; Kim K. S. *Phys. Rev. B* **2004**, *69*, 193404.
4. (a) Zhang, Z.; Sun, X.; Dresselhaus, M. S.; Ying, J. Y. *Phys. Rev. B* **2000**, *61*, 4850. (b) Bockrath, M.; Liang, W.; Bozovic, D.; Hafner, J. H.; Lieber, C. M.; Tinkham, M.; Park, H. *Science* **2001**, *291*, 283.
5. Carmona, F.; Barreau, F.; Delhaes, P.; Canet, R. *J. Phys. Lett.* **1980**, *41*, L-531.
6. (a) Hall, D. *Anal. Biochem.* **2001**, *288*, 109-125. (b) Schuck, P. *Annu. Rev. Biophys. Biomol. Struct.* **1997**, *26*, 541-566.
7. Kneipp, K.; Kneipp, H.; Itzkan, I.; Dasari, R. R.; Feld, M. S. *Chem. Rev.* **1999**, *99*, 2957.

8. Dresselhaus, M. S.; Dresselhaus, G.; Eklund, P. C. *Science of Fullerenes and Carbon Nanotubes*; Academic Press: New York, 1996.

9. (a)Tsang, S. C.; Davis, J. J.; Green, M. L. H.; Hill, H. A. O.; Leung, Y. C.; Sadler, P. J. *Chem. Commun.* **1995**, 1803. (b) Davis, J. J.; Green, M. L. H.; Hill, H. A. O.; Leung, Y. C.; Sadler, P. J.; Sloan, J.; Xavier, A. V.; Tsang, S. C. *Inorg. Chim. Acta* **1997**, *272*, 261. (c) Wong, S. S.; Joselevich, E.; Woolley, A. T.; Cheung, C. C.; Lieber, C. M. *Nature* **1998**, *394*, 52. (d) Baughman, R. H.; Cui, C.; Zakhidov, A. A.; Iqbal, Z.; Barisci, J. N.; Spinks, G. M.; Wallace, G. G.; Mazzoldi, A.; De Rossi, D.; Rinzler, A. G.; Jaschinski, O.; Roth, S.; Kertesz, M. *Science* **1999**, *284*, 1340. (e) Mattson, M. P.; Haddon, R. C.; Rao, A. M.; Mol. J. *Neurosci.* **2000**, *14*, 175.

10. (a) Martel, R.; Schmidt, T.; Shea, H. R.; Hertel, T.; Avouris, P. *Appl. Phys. Lett.* **1998**, *73*, 2447. (2) Wang, Q. H.; Setlur, A. A.; Lauerhaas, J. M.; Dai, J. Y.; Seelig, E. W.; Chang, R. P. H. *Appl. Phys. Lett.* **1998**, *72*, 2912. (c) Dillon, A. C.; Jones, K. M.; Bekkedahl, T. A.; Kinag, C. H.; Bethune, D. S.; Heben, M. J. *Nature* **1997**, *386*, 377. (d) Dai, H. J.; Hafner, J. H.; Rinzler, A. G.; Colbert, D. T.; Smalley, R. E. *Nature* **1996**, *384*, 147. (e) Yu, M. F.; Lourie, O.; Dyer, M. J.; Moloni, K.; Kelly, T. F.; Ruoff, R. S. *Science* **2000**, *287*, 637.

11. Ebbesen, T. W.; Ajayan P. M. *Nature* **1992**, *358*, 220.

12. Guo, T.; Nikolaev, P.; Thess, A.; Colbert, D. T.; Smally, R. E. *Chem. Phys. Lett.* **1995**, *243*, 49.

13. Kong, L.; Cassell, A. M.; Dai, H. J. *Chem. Phys. Lett.* **1998**, *292*, 567.

14. Pederson, M. R.; Broughton, J. Q. *Phys. Rev. Lett.* **1992**, *69*, 2689.

15. (a) Seshardri, R.; Govindaraj, A.; Aiyer, H. N.; Sen, R.; Subbanna, G. N.; Raju, A. R.; Rao, C. N. R. *Curr. Sci.* **1994**, *66*, 839. (b) Ajayan, P. M.; Iijima, S. *Nature* **1993**, *361*, 333.

16. (a) Liu, M.; Cowley, J. M. *Carbon* **1995**, *33*, 225. (b) Yosida, Y. *Appl. Phys. Lett.* **1994**,

32, 507.

17. Ajayan, P. M.; Colliex, C. ; Lambert, J. M.; Bernier, P.; Barbedette, L.; Tencé, M.; Stephan, O. *Phys. Rev. Lett.* **1994**, *72*, 1722.
18. (a) Guerret-Piécourt, C.; Le Bouar, Y.; Loiseau, A.; Pascard, H *Nature* **1994**, *372*, 761. (b) Loiseau, A.; Pascard, H *Chem. Phys. Lett.* **1996**, *256*, 246.
19. (a) Setlur, A. A.; Lauerhaas, J. M.; Dai, J. Y.; Chang, R. P. H. *Appl. Phys. Lett.* **1996**, *69*, 345. (b) Dai, J. Y.; Lauerhaas, J. M.; Setlur, A. A.; Chang, R. P. H. *Chem. Phys. Lett.* **1996**, *258*, 547.
20. Ugarte, D.; Châtelain, A. ; de Heer, W. A. *Science* **1996**, *274*, 1897.
21. Sloan, J.; Wright, D. M.; Woo, H.-G.; Bailey, S.; Brown, G.; York, A. P. E.; Coleman, K. S.; Hutchison, J. L.; Green, M. L. H. *Chem. Comm.* **1999**, 699.
22. Govindaraj, A.; Satishkumar, B. C.; Nath, M.; Rao, C. N. R. *Chem. Mater.* **2000**, *12*, 202.
23. Sun, X; Li, Y *Adv. Mater.* **2005**, *17*, 2626.
24. Wang, X. K. ; Lin, X. W. ; Mesleh, M. ; Jarrold, M. F. ; Dravid, V. P. ; Ketterson, J. B. ; Chang, R. P. H. *J. Mater. Res.* **1995**, *10*, 1.
25. Zhang, Y.; Suenaga, K.; Colliex, S.; Iijima, S. *Science* **1998**, *281*, 973.
26. (a) Seiler, H.; Hass, U.; Ocker, B.; Körtje, K.-H. *Faraday Discuss.* **1991**, *92*, 121. (b) Ding, D. J.; Li, H. M.; Pu, Q. R.; Zhang, Z. M. *Phys. Rev. B* **2002**, *66*, 085411.
27. Ann, C. C.; Krivanek, O. L. K.; Burgner, R. P.; Swann, P. R. *EELS Atlas;* Gatan: Warrendale, 1983.
28. Yu, D. P.; Xing, Y. J.; Tence, M.; Pan, H. Y.; Leprince-Wang, Y. *Physica E*, **2002**, *15*, 1.
29. (a) Wang, Y. W.; Hong, B. H.; Lee, J. Y.; Kim, J.-S.; Kim, G. H.; Kim, K. S. *J. Phys. Chem. B* **2004**, *108*, 16723. (b) Wang, J.; An, X.; Li, Q.; Egerton, R. F. *Appl. Phys. Lett.* **2005**, *86*, 201911.
30. Sun, Y.; Yin, Y. Mayer, B. T.; Herricks, T.; Xia, Y. *Chem. Mater.* **2002**, *14*, 4736.

31. Chen, Q.; Wang, S.; Peng, L.-M. *Nanotechnology* **2006**, *17*, 1087.

32. (a) Hu, J.; Odom, T. W.; Lieber, C. M. *Acc. Chem. Res.* **1999**, *32*, 435. (b) Loiseau, A.; Willaime, F. *Appl. Surf. Sci.* 2000, *164*, 227. (c) Hsia, C.-H.; Yen, M.-Y.; Lin, C.-C.; Chiu, H.-T.; Lee, C.-Y. *J. Am. Chem. Soc.* **2003**, *125*, 9940. (d) Huang, C.-H.; Chang, Y.-H.; Lee, C.-Y.; Chiu, H.-T. *Langmuir* **2006**, *22*, 10.

33. (a) Setlur, A. A.; Doherty, S. P.; Dai, J. Y.; Chang, R. P. H. *Appl. Phys. Lett.* **2000**, *76*, 3008. (b) Doherty, S. P.; Chang, R. P. H. *Appl. Phys. Lett.* **2002**, *81*, 2466. (c) Buchholz, D. B.; Doherty, S. P.; Chang, R. P. H. *Carbon* **2003**, *41*, 1625.

34. Gavillet, J.; Loiseau, A.; Ducastelle, F.; Thair, S.; Bernier, P.; Stéphan, O.; Thibault, J.; Charlier, J.-C. *Carbon* **2002**, *40*, 1649.

35. Karakaya, I.; Thompson, W. T. *Bulletin of Alloy Phase Diagrams*; American Society for Metals: Metals Park, Ohio, 1990.

36. Hulteen, J. C.; Martin, C. R. *J. Mater. Chem.* **1997**, *7*, 1075.